EUROPEAN JOURNAL OF Haematology

European Journal of Haematology 87 (312–322)

ORIGINAL ARTICLE

# Distribution of dystrophin- and utrophin-associated protein complexes (DAPC/UAPC) in human hematopoietic stem/progenitor cells

Carmen Teniente-De Alba[1], Ivette Martínez-Vieyra[2], Raúl Vivanco-Calixto[1], Iván J. Galván[3], Bulmaro Cisneros[2], Doris Cerecedo[1]

[1]Laboratorio de Hematobiología, Escuela Nacional de Medicina y Homeopatía, Instituto Politécnico Nacional (IPN), México, D.F., México; [2]Departamento de Genética y Biología Molecular; [3]Unidad de Microscopía Confocal, Centro de Investigación y de Estudios Avanzados (CINVESTAV) del IPN, México, D.F., México

## Abstract

Hematopoietic stem cells (HSC) are defined by their cardinal properties, such as sustained proliferation, multilineage differentiation, and self-renewal, which give rise to a hierarchy of progenitor populations with more restricted potential lineage, ultimately leading to the production of all types of mature blood cells. HSC are anchored by cell adhesion molecules to their specific microenvironment, thus regulating their cell cycle, while cell migration is essentially required for seeding the HSC of the fetal bone marrow (BM) during development as well as in adult BM homeostasis. The dystrophin-associated protein complex (DAPC) is a large group of membrane-associated proteins linking the cytoskeleton to the extracellular matrix and exhibiting scaffolding, adhesion, and signaling roles in muscle and non-muscle cells including mature blood cells. Because adhesion and migration are mechanisms that influence the fate of the HSC, we explored the presence and the feasible role of DAPC. In this study, we characterized the pattern expression by immunoblot technique and, by confocal microscopy analysis, the cellular distribution of dystrophin and utrophin gene products, and the dystrophin-associated proteins ($\alpha$-, $\beta$-dystroglycan, $\alpha$-syntrophin, $\alpha$-dystrobrevin) in relation to actin filaments in freshly isolated $CD34^+$ cells from umbilical cord blood. Immunoprecipitation assays demonstrated the presence of Dp71d/Dp71$\Delta_{110}{}^{m}$~DAPC and Up400/Up140~DAPC. The subcellular distribution of the two DAPC in actin-based structures suggests their dynamic participation in adhesion and cell migration. In addition, the particular protein pattern expression found in hematopoietic stem/progenitor cells might be indicative of their feasible participation during differentiation.

**Key words** dystrophin; utrophin; stem cells

**Correspondence** Dr. Doris A. Cerecedo Mercado, Laboratorio de Hematobiología, Escuela Nacional de Medicina y Homeopatía, I.P.N., Guillermo Massieu Helguera No. 239, Col. La Escalera Ticomán, 07320 México, D.F., México. Tel: (+52) (55) 5729 6300, ext. 55531; Fax: (+52) (55) 5729 6300, ext. 55532; e-mail: dcereced@prodigy.net.mx

Accepted for publication 25 May 2011

doi:10.1111/j.1600-0609.2011.01657.x

Blood cells are produced throughout life by a process termed hematopoiesis, which is defined as the expansion and differentiation of a very small population of pluripotent hematopoietic stem cells (HSC) in the bone marrow (BM). HSC give rise to a hierarchy of progenitor populations with more restricted potential lineage, ultimately leading to the production of all types of mature blood cells. Therefore, the hematopoietic system is a privileged observatory for the study of the highly coordinated process leading to cell differentiation. Hematopoietic stem and progenitor cells differentiation is controlled by the combined effects of hematopoietic growth factors (HGFs), chromatin modifiers, transcription factors, and microRNAs (miRNAs) (1). Upon the appropriate stimuli, migration of HSC occurs across the endothelial vasculature to different organs and to their

appropriate niche within the BM cavity, a process termed homing. Homing is a coordinated, multistep process that involves signaling growing factors, activation of receptors, and cytoskeleton rearrangements, leading to the formation of a lamellipodium at the front side and a uropod at the rear (2).

Because cell–extracellular matrix adhesion is a prerequisite for cell survival and also a key factor for differentiation of stem cells, the identification and characterization of protein complexes involved in this process are necessary steps to understand lineage-specific cell function and to develop clinical applications for these cells. In this respect, the dystrophin-associated protein complex (DAPC) – a large membrane-spanning multiprotein complex comprising dystrophin/utrophin, sarcoglycans, dystroglycans, dystrobrevins, and syntrophins (3) – modulates cell adhesion and intracellular signal transduction in numerous terminal-differentiated cell types by providing a connection between the extracellular matrix and the intracellular cytoskeleton (4, 5). In our previous studies, we identified the presence of DAPC in different mature blood cell types, including platelets and neutrophils, and provided evidence for DAPC participation in cell adhesion. In platelets, DAPC may modulate adhesion by participating as scaffolding protein complex (6, 7), while in neutrophils, DAPC might be involved in cytoskeleton reorganization during chemotaxis (8). In this study, we reported, to our knowledge for the first time, the expression and subcellular distribution profile of DAPC members in HSC from umbilical cord blood by using confocal microscopy and Western blot analyses. Furthermore, we demonstrated by immunoprecipitation assays the conformation of at least two DAPC in these cells, Dp116/Dp71d/Dp71$\Delta_{110}{}^{m}$~DAPC and Up400/Up140~DAPC, and provide evidence for their participation in cell migration.

## Methods

### Antibodies

Table 1 lists the recognition properties of all of the antibodies used in this study. Monoclonal and polyclonal are referred as (mAbs) and (pAbs), respectively.

### Cell source

Umbilical cord blood (CB) units were obtained by donation from the Centro Nacional de la Transfusión Sanguínea in Mexico City at the end of full-term deliveries, after clamping and cutting of the cord by drainage of blood into sterile collection tubes containing the anticoagulant citrate-phosphate.

### $CD34^+$ cell purification

Mononuclear cells were separated from CB by Ficoll-Paque (Amersham Pharmacia Biotech, Uppsala, Sweden) density gradient centrifugation (9). After washing twice, aliquots of the cells were employed for isolation of $CD34^+$ cells, and for phenotypic analysis, $CD34^+$ cells were enriched using a $CD34^+$ Progenitor Cell Selection System (Dynal AS, Oslo, Norway) according to the manufacturer's instructions, which yielded 95% pure $CD34^+$ according to the flow cytometric evaluation performed after blocking surface Fc receptors and after their incubation with FITC-conjugated anti-CD34 monoclonal antibodies (Santa Cruz Biotechnology Inc., Santa Cruz, CA, USA), after which two-color flow cytometry was utilized to assess co-expression of cell surface antigens with CD34. This analysis was performed in a FACS Calibur flow cytometer using CELLQUEST software (Becton Dickinson Labware, Franklin Lakes, NJ, USA) with the acquisition of at least 10 000 events for each sample. Surface expression of antigens was evaluated employing

**Table 1** Characteristics of the different antibodies used in this study

| Antibody | Position of antigen | Specificity | Reference/resource |
|---|---|---|---|
| H4 pAb | C-T last 11 aa | Dp427, Dp260, Dp140, Dp116, Dp71 | (30) |
| Dys2 mAb | C-T last 17 aa | Dp427, Dp260, Dp140, Dp116, Dp71 | Novocastra (New Caste, UK) |
| Utrophin 3B6 mAb | Peptide 261–371 human utrophin | Up400 | Sta. Cruz Biotechnology Inc. (CA, USA) |
| K7 pAb | C-T last 15 aa | Up400, Up140, Up71 | (30) |
| β-Dystroglycan L-20 pAb | Peptide C-T | β-Dystroglycan | Sta. Cruz Biotechnology Inc. (CA, USA) |
| JAF pAb | C-T last 7 aa | β-Dystroglycan | (31) |
| α-syntrophin pAb | Peptide C-T | α-syntrophin | Sta. Cruz Biotechnology Inc. (CA, USA) |
| α-syntrophin pAb | Peptide 191–206 | α-syntrophin | (31) |
| α-dystrobrevin pAb | C-T last 19 aa | α-dystrobrevin | Sta. Cruz Biotechnology Inc. (CA, USA) |
| α-actin mAb | C-T aa human origin | Actin | Sta. Cruz Biotechnology Inc. (CA. USA) |

mAb, monoclonal antibody; pAb, polyclonal antibody.

the following antibodies: anti-CD34-FITC (hematopoietic progenitor/stem cell); CD38-Phycoerythrin (PE) (immature subset) (Santa Cruz Biotechnology Inc.). As the $CD34^+$ fraction is rather heterogeneous and only a small amount of this population are true HSCs; $CD34^+$ cells are considered hematopoietic stem/progenitor cells (HSPCs).

### $CD34^+$ cultures

Two to 10 000 CD34/CB cell-isolated $CD34^+$ cells from human umbilical CB were cultured in quadruplicate, flat-bottomed, 24-well plates in 1 mL IMDM supplemented with 10% FCS in the presence of FLT3 (50 ng/mL), and TPO (10 U/mL) (Preprotech, Rocky Hill, NJ, USA) in microwells twice a week. The wells were grown at 37°C for 3 wks with 5% of $CO_2$.

### Immunofluorescence staining (IF)

$CD34^+$ cells were seeded on poly-L-lysine-coated coverslips and after 20 min were fixed for 20 min with 2% paraformaldehyde/PBS and 0.04% NP40 in the cytoskeleton-stabilizing solution PHEM (100 mM PIPES, 5.25 mM HEPES, 10 mM EGTA, 20 mM $MgCl_2$, pH 6.9) (Sigma Chemical Co., St. Louis, MO, USA) and for 1 h with 2% paraformaldehyde. HSPCs cells were first incubated for 1 h with 0.1 $\mu$g/mL phalloidin, tetramethylrhodamine B isothiocyanate (TRITC) (Sigma Chemical Co.) to label actin filaments and was then incubated for 2 h with the appropriate primary antibodies (Table 1) diluted in 0.1% fetal bovine serum (FBS) in PBS. Cells were washed with PBS and incubated for 1 h with the secondary anti-mouse, anti-rabbit, or anti-goat antibodies conjugated to Alexa-Fluor-568 or Alexa-Fluor-488 (Molecular Probes, Eugene, OR, USA), washed, and mounted in Vectashield media (Vector Laboratories Inc., Burlingame, CA, USA). Slides were observed using a Leica confocal instrument model TCS-SP5 Mo, and images were taken at 63× at zoom 3 at 1024 × 1024 pixels with an HCX PL APO 63X/1.40–0.60 DIL CS oil immersion. Optical sections [z] were captured at 0.18 $\mu$m. Negative controls included cells incubated with an irrelevant polyclonal antibody or cells just exposed to the fluorescent-secondary antibodies. None of these controls showed any conspicuous signal. It is important to note that the antibody chosen for this analysis corresponded to the one that better let visualize the corresponding images.

### Western blot analysis

Homogenates were sonicated, and protein concentrations were determined by the Bradford method (Bio-Rad, Hercules, CA, USA). A portion (50 $\mu$g) of protein extract was mixed with an equal volume of 2X sample buffer [50 mM Tris–HCl (pH 6.8), 15% (w/v) SDS, 5% (v/v), $\beta$-mercaptoethanol, 20% (v/v) glycerol, 0.1% (w/v) bromophenol blue] and boiled for 3 min. Proteins were resolved by SDS–PAGE (10% (w/v) and electrotransferred onto nitrocellulose membrane, using a semidry system (Thermo Fisher Scientific Inc., Waltham, MA, USA). Membranes were incubated with the appropriate primary antibodies and then with horseradish peroxidase-conjugated secondary antibodies, visualized using an enhanced chemiluminescence Western blot analysis system (Santa Cruz Biotechnology Inc.), and documented utilizing X-omat film (Kodak, Rochester, NY, USA). Antibodies used for this assay corresponded to those that offer a well-known good performance in Wb. Negative controls consisted of transferred strips incubated only with horseradish peroxidase-conjugated secondary antibodies.

### Immunoprecipitation assays

$CD34^+$ cells were resuspended in 50 mM Tris–HCl (pH 8) containing complete Protease Inhibitor Cocktail (Roche, Mannheim, Germany). Homogenates were sonicated with an equal volume of 2X RIPA buffer (10 mM 9 Tris–HCl (pH 7.4), 1 mM EGTA, 158 mM NaCl, 10 mM $Na_3MoO_4$, 25 mM NaF, 1 mM phenylmethanesulphonyl fluoride, 1 mM EDTA, 2 mM $Na_3VO_4$). After determination of protein concentration by the Bradford method, cell lysates were added to an equal volume of ice-cold RIPA buffer containing 1% (w/v) Triton X-100 and 0.1% (w/v) SDS. Lysates were incubated for 2 h at 4°C with the appropriate immunoprecipitating antibodies (Table 1) and subsequently incubated overnight with Protein G plus sepharose (Santa Cruz Biotechnology Inc.). Immunoprecipitates (Ip) were separated by centrifugation, washed with lysis buffer, resuspended in 2X sample buffer, and then boiled for 5 min. Immunoprecipitated proteins were analyzed by Western blot, as described previously. It is important to note that to avoid the visualization of immunoglobulin heavy chain band that could interfere with the band of interest, different species antibodies were chosen between the immunoprecipitating antibody and the Wb antibody.

## Results

### Dystrophin proteins are present in HSPCs and co-localize with actin filaments

To identify the expression pattern of dystrophin proteins in HSPCs, we carried out Western blot assays using the anti-dystrophin antibody H4, directed against epitopes localized in the dystrophin C-terminal region (Table 1).

Because muscle cells express the majority of dystrophin family members, the mouse muscle cell line C2C12 was employed as positive control.

The anti-dystrophin antibody H4 revealed the presence of only three bands in HSPCs extracts; of these three, the two bands with slow mobility co-migrated toward those found in the C2C12 non-differentiated cell extract. Dp71 is expressed in all tissues, except for skeletal muscle, where its expression is exclusively confined to myoblasts (10–12); on the contrary, Dp427 is the major isoform expressed in mature fibers (13, 14). The upper band with a relative molecular weight of 116 kDa may correspond to Dp116, while the middle band with a predicted molecular weight of 76 kDa must correspond with Dp71d. Finally, a faint band of approximately 55 kDa that was evident only in HSPCs extracts might correspond to $Dp71\Delta_{110}{}^{m}$ (Fig. 1A). Dp71 transcripts are alternatively spliced in exons 71–74 and 78 to produce multiple products of 70–78 kDa; Dp71d preserves the C-terminal, while $Dp71\Delta_{110}{}^{m}$ is the result of the alternatively splicing at exons 71–74 and/or 78 (15).

To evaluate the subcellular distribution of dystrophin proteins, immunofluorescence confocal microscope analysis on $CD34^{+}$ cells was performed. Because the H4 antibody recognizes the C-terminal region of dystrophin that is shared among Dp116, $Dp71\Delta_{110}{}^{m}$, and Dp71d, the distribution observed is referred to as Dps (Fig. 1B). In $CD34^{+}$ cells, Dps immunostaining displayed a punctuated pattern distributed at the plasma membrane, cytoplasm, and nucleus, which co-localized to a certain extent with that observed for actin filaments in the cell membrane and nucleus (Fig. 1B). A fourth line merging green and red labels only was included to observe the respective proteins distribution. Negative controls were performed using only the FITC secondary antibody (data not shown).

### Utrophins are present in CD34+ cells and are co-distributed with actin filaments

The presence of utrophin family proteins in HSPCs $CD34^{+}$ was ascertained by immunoblotting analysis utilizing the K7 antibody, directed against the last C-terminal 15 aa of Up400 (Table 1). Immunoreactive bands that might correspond to Up400 and to Up140 were revealed in both C2C12 and HSPCs cell extracts, while a lower band with a relative molecular mass of 76 kDa

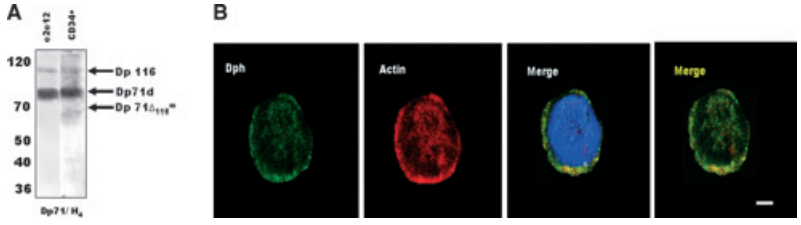


**Figure 1** Identification and cellular distribution of short dystrophins in human hematopoietic stem/progenitor cells (HSPCs). (A) Whole lysates, obtained from C2C12 cells and HSPCs ($CD34^{+}$), were analyzed by Western blot using the H4 anti-dystrophin antibody. Dystrophin isoforms detected with antibody H4 were identified as Dp116 (115 kDa), Dp71d (76 kDa), and $Dp71\Delta_{110}{}^{m}$ (55 kDa) (arrows). Migration of protein markers is shown on the left. (B) Hematopoietic stem cells were seeded on glass cover slips and immunostained with the primary anti-dystrophin antibody H4, and the specific signal for Dp116/Dp71d/$Dp71\Delta_{110}{}^{m}$ was developed using a secondary fluorescein-conjugated antibody (green color). Cells were counterstained with DAPI (blue color) and rhodamine-conjugated phalloidin (red color) to visualize nuclei and cytoplasmic actin, respectively. After triple labeling, cell preparations were subjected to confocal microscopy analysis. Merged images are shown on the right panels. Scale bar = 1.5 $\mu$m.

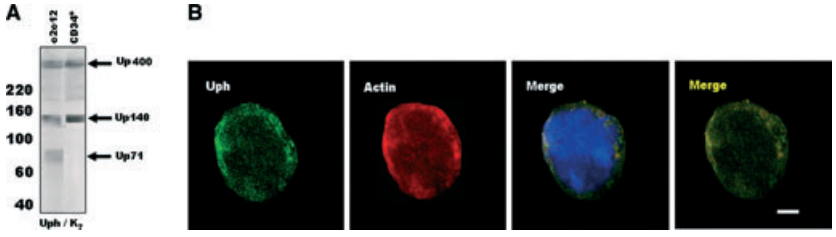


**Figure 2** Expression and distribution of utrophin gene products in human hematopoietic stem/progenitor cells (HSPCs). (A) To identify utrophin isoforms expressed in hematopoietic stem cells (HSC), Western blot analysis of whole lysates from C2C12 cells and human HSPCs $CD34^{+}$ was carried out. Up400 (395 kDa) and Up140 (140 kDa) were revealed with the anti-utrophin antibody K7 (arrows). Migration of protein markers is shown on the left. (B) HSC ($CD34^{+}$) were analyzed by immunofluorescence and confocal microscopy employing the primary anti-utrophin antibody K7, and the specific signals for Up400/Up140 were developed with a secondary fluorescein-conjugated antibody (green color). Cells were counterstained with DAPI (blue color) and rhodamine-conjugated phalloidin (red color) to visualize nuclei and actin filaments, respectively. Merged images are shown in the right panels. Scale bar = 1.5 $\mu$m.

that may correspond to Up71 was detected solely in the C2C12 non-differentiated cell extract (Fig. 2A). Up71 is expressed in myoblasts and unlike dystrophin, it is only increased 2-fold during myogenic differentiation (9, 16, 17).

Cellular distribution of utrophins was ascertained in $CD34^+$ cells utilizing the anti-utrophin antibody K7. Up400/Up140, referred to as Ups, were distributed mainly at the plasma membrane with scarce presence in the cytoplasm. Ups co-localized with F-actin mainly at the plasma membrane and to a lesser extent in the nucleus (Fig. 2B). A fourth line merging green and red labels only was included to observe the respective proteins distribution. Negative controls were performed using the FITC secondary antibody alone (data not shown).

### DAP are present in $CD34^+$ cells

To ascertain the presence of dystrophin-associated proteins (DAP) in HSPCs, specific antibodies directed against each DAP analyzed (α-dystroglycan, β-dystroglycan, α-syntrophin, and α-dystrobrevin) were employed for immunoblotting and immunofluorescence assays. In HSPCs cell extracts, the anti-α-dystroglycan revealed the presence of three immunoreactive bands with relative molecular mass of 156, 120, and 80 kDa, with the upper band the only band shared between HSPCs and C2C12 non-differentiated cell extracts. Co-migrated immunoreactive bands corresponding to β-dystroglycan were found in HSPCs (52 kDa) and C2C12 (43 kDa) extracts, while immunoreactive bands of 84 and 56 kDa that must correspond to α-dystrobrevin-1 and α-syntrophin, respectively, were found in both HSPCs and control extracts (Fig. 3A).

Distribution of DAP was analyzed by immunofluorescence assays. In $CD34^+$ cells, α-dystroglycan immunolabeling was discontinuous with discrete aggregates at the plasma membrane and displayed scarce co-localization with actin filaments in this cell region (Fig. 3B). Beta-dystroglycan immunostaining was homogenously distributed throughout the entire cell body with some intensely stained nuclear bodies and showed co-localization with actin labeling at the cell periphery and nucleus (Fig. 3B).

Apparently, α-dystroglycan and β-dystroglycan did not have the same distribution which might be attributable to the different z stacks observed in the figure.

On the other hand, α-syntrophin exhibited a granular immunolabeling pattern homogeneously distributed throughout the cell that co-localized with actin, mainly in the nucleus (Fig. 3B, merge). Finally, the α-dystrobrevin antibody revealed a homogeneous distribution of the protein encompassing the cytoplasm and nuclei with some intensely stained aggregates; co-localization between α-dystrobrevin and actin filaments was evident in most of the cell body (Fig. 3C, merge). A fourth line merging green and red labels only was included to observe the respective proteins distribution. Negative controls were performed using the FITC secondary antibody alone (data not shown).

### Dystrophins and utrophins are co-distributed with DAP in $CD34^+$ cells

To ascertain the potential association of Dp116/Dp71d/$Dp71\Delta_{110}{}^m$ or Up400/Up140 with DAP (β-dystroglycan, α-syntrophin, and α-dystrobrevin) in HSPCs, we analyzed as a first step whether these proteins co-localize by confocal microscopy assays. Immunofluorescence images show that both Dp116/Dp71d/$Dp71\Delta_{110}{}^m$ (Fig. 4A) and Up400/Up140 (Fig. 4B) co-localized with β-dystroglycan and α-syntrophin mainly in the cell periphery, and with α-dystrobrevin throughout the cell (Fig. 4A). A fourth line merging green and red labels only was included to observe the respective proteins distribution. Negative controls were performed using the TRITC secondary antibody alone (data not shown).

Altogether, these results suggest the conformation of DAPC in HSPCs that contain Dp116/Dp71d/$Dp71\Delta_{110}{}^m$ or Up400/Up140 as core proteins.

### Dystrophins and utrophins make up DAPC in $CD34^+$ cells

To demonstrate directly the interaction between Dp116/Dp71d/$Dp71\Delta_{110}{}^m$, or actin with DAP in HSPCs cells, immunoprecipitation assays were carried out using immunoprecipitating antibodies, Dys2 against Dp116/Dp71d/$Dp71\Delta_{110}{}^m$, utrophin 3B6 for Up400/Up140, or actin. Co-immunoprecipitated proteins (Ip) were analyzed by immunoblotting with antibodies against actin, DAP, dystrophins (H4), and utrophins (K7). Immunoprecipitation of actin pulled down dystrophins Dp71 (76 kDA) and $Dp71\Delta_{110}{}^m$ (55 kDa), utrophins Up400 (395 kDa) and Up140 (140 kDa), α-dystrobrevin-1 (84 kDa) (Fig. 5A), β-dystroglycan (52 and 43 kDa bands), and α-syntrophin (59 kDa). An additional band of unknown origin was observed in the α-syntrophin immunoprecipitation assay.

Immunoprecipitation assays for Dp116/Dp71d/$Dp71\Delta_{110}{}^m$ were performed with the anti-dystrophin antibody Dys2. Together with dystrophins, β-dystroglycan (43 and 52 kDa), α-syntrophin (58 kDa), α-dystrobrevin-1 (84 kDa), and actin (42 kDa) were co-immunoprecipitated from $CD34^+$ cells (Fig. 5B). When Up400/Up140 was immunoprecipitated using the K7 antibody, β-dystroglycan (43 and 52 kDa), α-syntrophin (58 kDa), α-dystrobrevin-1 (84 kDa), and actin (42 kDa) were co-purified from CD $34^+$ cells (Fig. 5C).

Altogether, these results show the existence of two alternative protein complexes in $CD34^+$ cells, which are

 

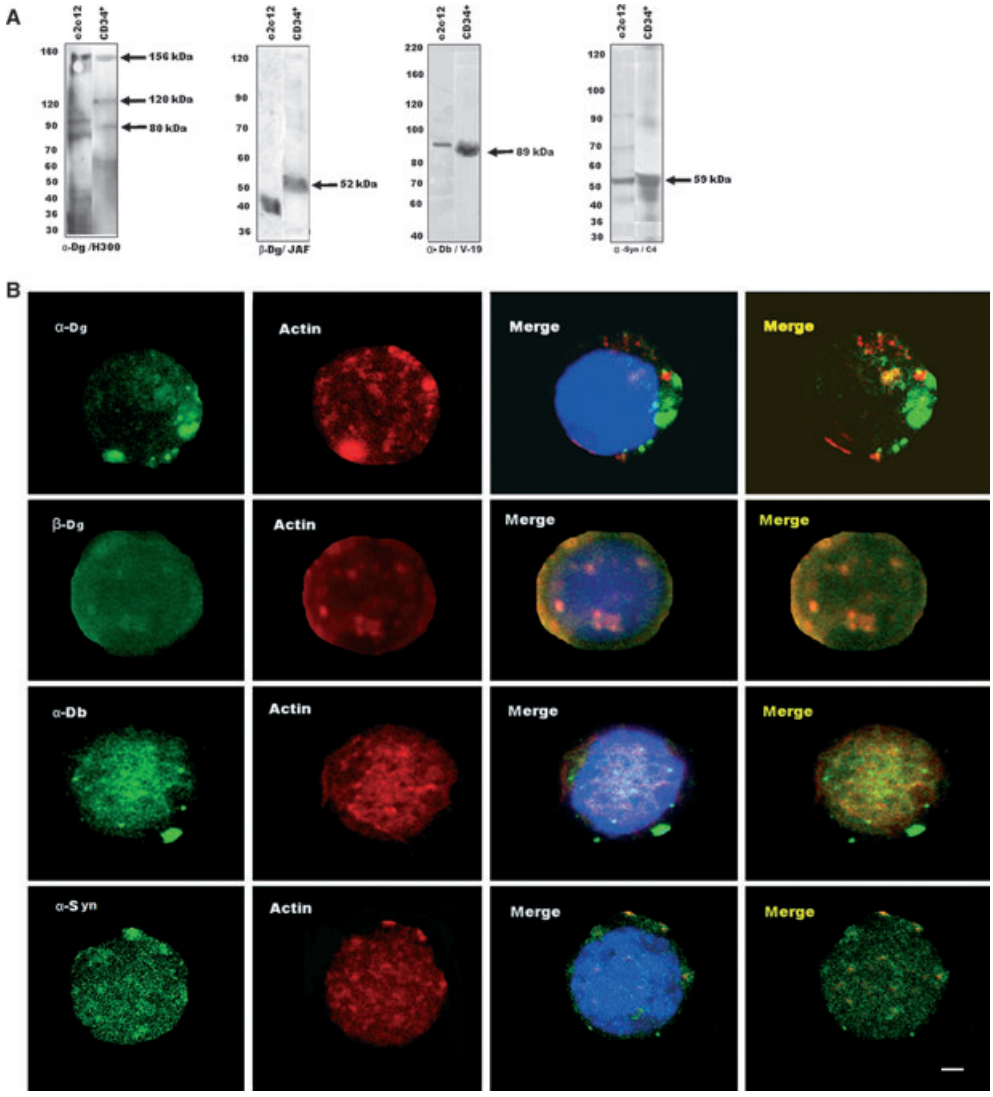


**Figure 3** Identification and distribution of dystrophin-associated protein (DAP) and actin in human hematopoietic stem/progenitor cells (HSPCs). (A) Whole protein lysates from C2C12 cells and from human HSPCs ($CD34^+$) were comparatively analyzed by immunoblotting. Blots were immunostained with antibodies against α-dystroglycan (α-dg), β-dystroglycan (β-dg), α-dystrobrevin (α-db), and α-syntrophin (α-syn). Arrows on the right denote the specific protein bands for α-dystroglycan (156 and 120 kDa) for $CD34^+$ cells and 156 kDa for C2C12, β-dystroglycan (52 and 43 kDa for C2C12), α-Db-1 (89 kDa) and α-syntrophin (59 kDa). (B) Confocal microscopy analysis of $CD34^+$ cells were carried out with primary antibodies direct to α-dystroglycan, β-dystroglycan, α-syntrophin, and α-dystrobrevin, and the specific signal for each protein was developed using a secondary fluorescein-conjugated antibody (green color). Counterstaining with DAPI (blue color) and rhodamine-conjugated phalloidin (red color) was carried out to stain nuclei and actin filaments, respectively. Merging images are shown on the right panels. Scale bar = 1.5 μm.

made up of Dp116/Dp71d/Dp71$\Delta_{110}{}^{m}$ or Up400/Up140 and their associated proteins. Furthermore, our data provided evidence of the interaction of these complexes with the actin cytoskeleton.

### Dystrophin-associated proteins participate during the migration process

One of the hallmarks of HSPCs is their migration, which show multiple podia when they are maintained in culture (18). Therefore, we obtained $CD34^+$ cell cultures and processed these by double immunofluorescence confocal microscopy, and analysis by flow cytometry revealed the presence of 87% of $CD34^+$ $CD38^-$ HSPCs (data not shown). Primary antibodies against dystrophins (Dph), utrophins (Uph), β-dystroglycan (β-dg), α-syntrophin (α-syn), and α-dystrobrevin (α-db) were revealed using FITC secondary antibodies, while actin filaments were revealed employing TRITC-phalloidin.

 

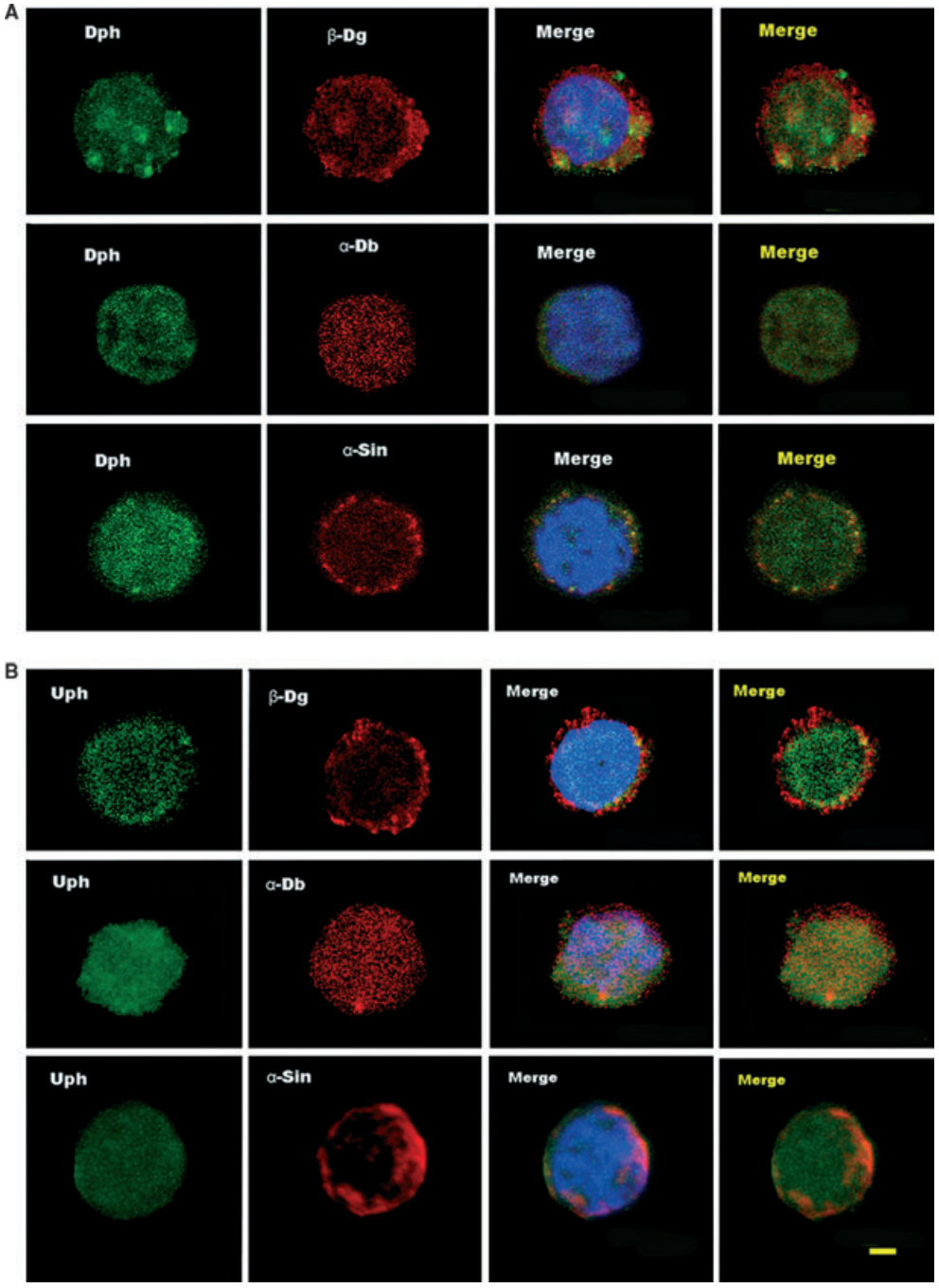


**Figure 4** Co-localization of dystrophins and utrophins with dystropin-associated proteins (DAP) in human hematopoietic stem/progenitor cells (HSPCs). (A) HSPCs were stained for Dp116/Dp71d/Dp71$\Delta_{110}^{m}$ using the anti-dystrophin antibody H4 and co-stained either anti-$\beta$-dystroglycan ($\beta$-dg), $\alpha$-dystrobrevin ($\alpha$-db), or anti-$\alpha$-syntrophin ($\alpha$-syn) antibody (DAP). Developing of Dp116/Dp71d/Dp71$\Delta_{110}^{m}$ was carried out with a secondary fluorescein-conjugated antibody (green color) while developing of each DAP was performed with a secondary rhodamine-conjugated antibody (red color). DAPI (blue color) was used to stain the nuclei. Scale bar = 1.5 $\mu$m. B. HSPCs were double immunolabeling with the anti-utrophin antibody K7 and either anti-$\beta$-dystroglycan ($\beta$-dg), $\alpha$-dystrobrevin ($\alpha$-db), or anti-$\alpha$-syntrophin ($\alpha$-syn) antibody. Developing of Up400/Up140 staining was carried out with a secondary fluorescein-conjugated antibody (green color) while developing of each DAP staining was performed with a secondary rhodamine-conjugated antibody (red color), and nuclei were identified with DAPI (blue color). Scale bar = 1.5 $\mu$m.

Dystrophins and utrophins demonstrated a polarized immunostaining pattern decorating the uropod and exhibited certain co-localization with actin. Distribution of DAP $\beta$-dystroglycan ($\beta$-dg), $\alpha$-syntrophin ($\alpha$-syn), and $\alpha$-dystrobrevin ($\alpha$-db) was also evident at the uropod, cellular protrusions, and regions where filamentous actin

 

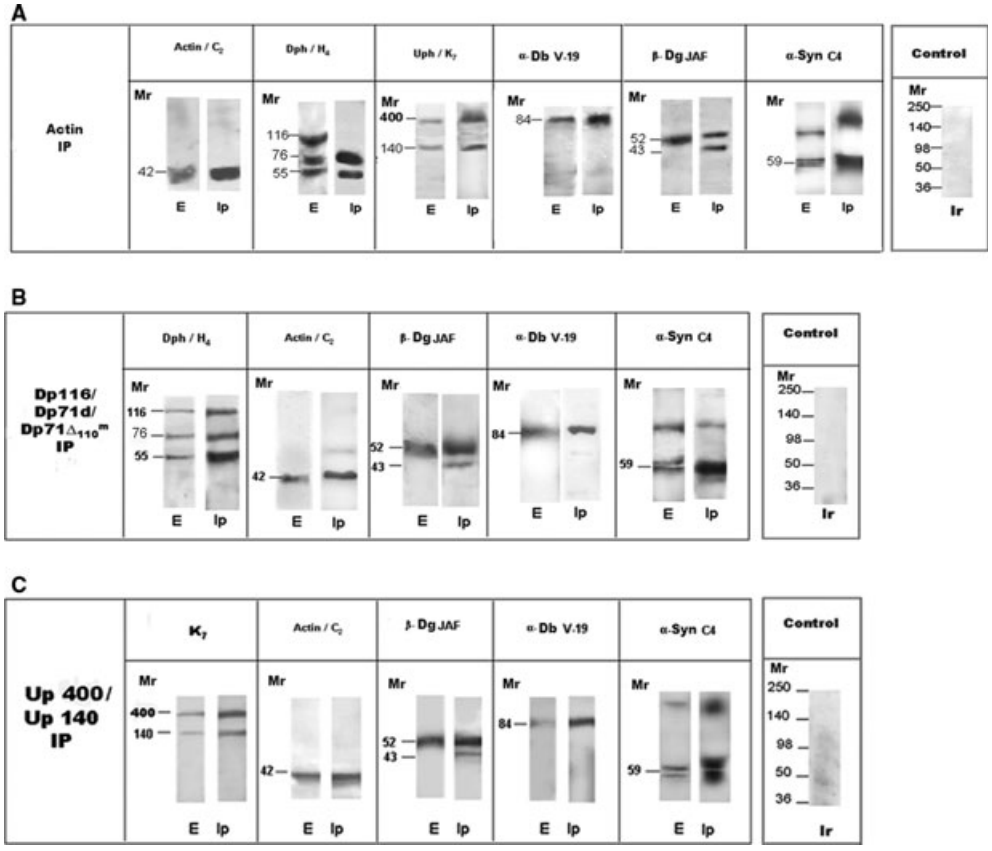


**Figure 5** Dystrophins and utrophins form protein complexes with dystropin-associated proteins (DAP) in human hematopoietic stem/progenitor cells (HSPCs). Protein extracts from $CD34^+$ cells were immunoprecipitated with anti-actin antibody (A), anti-Dp116/Dp71d/$Dp71\Delta_{110}^m$ (Dys2 antibody) (B) or anti-utrophin (utrophin 3B6 antibody) (C). Proteins from total extracts (E) and immunoprecipitates (Ip) were analyzed by Western blot using antibodies against actin, β-dystroglycan, α-syntrophin, α-dystrobrevin, Dp116/71d/$Dp71\Delta_{110}^m$ (H4 antibody), and Up400/Up140 (K7 antibody). Migration of protein markers is shown on the left. Controls treated with an irrelevant antibody are shown at the right.

staining was polarized (Fig. 6, arrows). Altogether, our results strongly suggest that dystrophin-associated proteins might participate as a scaffold for cytoskeleton remodeling, forming actin-based structures during cellular migration.

## Discussion

Mature blood tissue cells have a limited life span and are continuously replaced by the proliferation and differentiation of the HSC, which undergo constant renewal and consequently have an active regenerative compartment.

The signals that influence cell cycle and migratory status depend on the crosstalk among multiple ligand-receptor signaling pathways, which include adhesion molecules. Based on our previous studies on platelets and neutrophils related with the DAPC (7, 8), we were very interested in exploring the presence of these proteins in the hematopoietic stem-progenitor cells (HSPCs) and their feasible participation in adhesion and migration process.

In this study, we described, to our knowledge for the first time, the pattern of expression and subcellular localization of dystrophin (Dp116, Dp71d, and $Dp71\Delta_{110}^m$) and utrophin (Up400 and Up140) isoforms, as well as that of the DAP (α-, β-dystroglycan, α-syntrophin, and α-dystrobrevin-1) using Immunofluorescence (IF) and immunoblotting analyses. Furthermore, we demonstrated by immunoprecipitation assays the existence of alternative DAPC, which are composed of Dp71d/$Dp71\Delta_{110}^m$ or Up400/Up140 and β-dystroglycan, α-syntrophin, and α-dystrobrevin-1.

Dp116 protein was not present in actin immunoprecipitates, which can be attributed to its absence of actinbinding domains (19); however, it might be part of the cytoskeleton by its feasible indirect interaction with actin through β-dystroglycan as has been described in Scwann cells (20, 21).

 

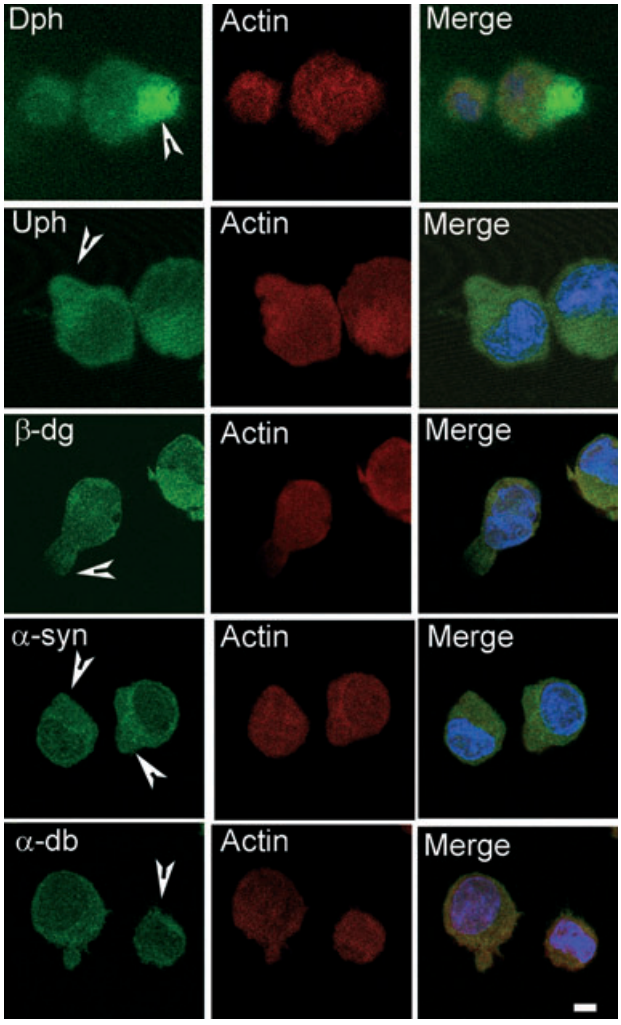


**Figure 6** The dystrophin- and utrophin-associated proteins are part of actin-based structures cultured human hematopoietic stem/progenitor cells (HSPCs). The feasible scaffolding role of the dystrophin, utrophin, and associated proteins were observed in HSPCs cultured and processed for double immunofluorescence staining and analyzed for confocal microscopy using the primary anti-dystrophin (H4), anti-utrophin (K7), anti-$\beta$-dystroglycan ($\beta$-dg), anti-$\alpha$-syntrophin ($\alpha$-syn), or $\alpha$-dystrobrevin ($\alpha$-db) developed with a secondary fluorescein-conjugated antibody (green color). Cells were counterstained with DAPI (blue color) and rhodamine-conjugated phalloidin (red color) to visualize nuclei and actin filaments, respectively. Merged images are shown on the right panels. Arrows denote plasma membrane protrusions of migrating cells. Scale bar = 2.5 $\mu$m.

In agreement with our results, it turns out interesting to consider that all this proteins and complexes might have redundant or complementary functions and certainly there must be a spatio-temporal regulation of their functions through mechanisms that remain to be elucidated as it seems unfeasible that they could operate simultaneously through the cell.

According to our results, we are required to consider the presence of DAPC as a scaffolding protein complex that has been initially recognized in muscular and non-muscular systems. In this regard, the presence of DAPC elements in cultured $CD34^+$ cells forming in actin-based structures such as filopodia, lamellipodia, and uropods confirms the role of DAPC as cytoskeleton elements involved in cell migration.

The fate of HSC and progenitor cells is determined by dynamic crosstalk among niche-originating cytokines, chemokines, and adhesion molecules. Cell adhesion molecules such as N-cadherin, $\beta$1-integrin, and osteopontin might not only be required for HSC anchoring to the niche, but also for involvement in the regulation of the cell cycle status of HSC (22). Considered dystroglycan as a cell adhesion molecule, it represents a physical connection between extracellular matrix and cytoskeleton, and it is a key transducer of signals from outside to inside. According to these assumptions, it is possible that in HSPCs $\alpha$-dystroglycan might participate in anchoring to niche components such as laminin and may participate in modulating cell functions inherent to the adhesion process including regulation of asymmetric cell division, as has been observed in Drosophila germline stem cells (23).

Previous reports have shown that signaling through Tie2/Ang-1 or Mpl/THPO induces $\beta$1-integrin- and N-cadherin-dependent HSC adhesion. Therefore, it is thought that $\beta$1-integrin and N-cadherin are key downstream targets of signaling in HSC (24, 25). In platelets, we have found DAPC and $\beta$1-integrin in close association with elements of focal adhesion complex and stress fiber organization. In addition, we have described $\beta$-dystroglycan as a key element in cytoskeleton remodeling, as has been recently reported in myoblasts (26). Therefore, it is tempting to speculate that DAPC via $\beta$-dystroglycan possesses a role in the adhesion, and ultimately in the differentiation process of HSPCs.

$\beta$-dystroglycan is required to polarize epithelial cells and the oocyte in Drosophila (27), while its knockdown induces death of the embryo. In these regard, the present results clearly show DAPC elements with a polarized pattern during $CD34^+$ cells migration.

It is noteworthy that the differential protein expression pattern reported here compared with that shown by mature cells (platelets and neutrophils) for certain elements such as $\beta$-dystrobrevin-2 and Up71, as well as the downregulated expression of others such as Dp116 might suggest their specific role in the differentiation stages.

In relation to the variation of the relative molecular weights between the $\beta$-dystroglycan of 52 kDa evidenced for $CD34^+$ cells compared with C2C12 co-migrated control (43 kDa) and that observed for the platelets of 43 kDa and 64 kDa found in neutrophils,

 

this could be attributed to the extent of their glycosylation. This dynamic differential expression reflects their diverse role during the proliferation and differentiation of the HSC and is related with their diverse binding patterns and functional properties (26). It is also noteworthy that our confocal microscopy analysis showed a strong presence of actin filaments and DAPC elements at HSC nuclei, as has been reported previously for C2C12 muscle cells. These findings suggest that DAPC are involved in nuclear structure and thereby might modulate nuclear processes (28), and that during the differentiation process they might control the gene expression regulating chromatin dynamics. As DAPC apparently diminishes their nuclear presence in mature forms such as neutrophils, their regulating role during the differentiation process is reinforced, as recently has been suggested in neurons (29). Study of the nuclear function of Dp71 and DAP in $CD34^+$ cells is currently in process at our laboratory.

In summary, this study provides evidence for the importance of DAPC in the migration and adhesion responses of HSPCs, and the performance of this type of study on HSPCs might promote the progress in the analysis of HSC biology and functional properties, contributing to their efficient expansion and to their clinical use in regenerative medicine.

## Acknowledgements

We thank Dr. Efrén Montaño, QFB Angélica Gómez, QFB Miriam Millán, and QFB. Silvia Tovar, QFB Sandra Ramírez and QFB Cristina Catañeda from the Centro Nacional de la Transfusión Sanguínea in Mexico City for the facilities given to obtain cord blood units.

## References

1. Weissman IL, Shizuru JA. The origins of the identification and isolation of hematopoietic stem cells, and their capability to induce donor-specific transplantation tolerance and treat autoimmune diseases. *Blood* 2008;**112**:3543–53.
2. Wright DE, Wagers AJ, Gulati AP, Johnson FL, Weissman IL. Physiological migration of hematopoietic stem and progenitor cells. *Science* 2001;**294**:1933–6.
3. Yoshida M, Suzuki A, Yamamoto H, Noguchi S, Mizuno Y, Ozawa E. Dissociation of the complex of dystrophin and its associated proteins into several unique groups by n-octyl beta-D-glucoside. *Eur J Biochem* 1994;**222**:1055–61.
4. Blake DJ, Weir A, Newey SE, Davies KE. Function and genetics of dystrophin and dystrophin-related proteins in muscle. *Physiol Rev* 2002;**82**:291–329.
5. Batchelor CL, Winder SJ. Sparks, signals and shock absorbers: how dystrophin loss causes muscular dystrophy. *Trends Cell Biol* 2006;**16**:198–205.
6. Cerecedo D, Martinez-Rojas D, Chavez O, Martinez-Perez F, García-Sierra F, Rendon A, Mornet D, Mondragón R. Platelet adhesion: structural and functional diversity of short dystrophin and utrophins in the formation of dystrophin-associated-protein complexes related to actin dynamics. *Thromb Haemost* 2005;**94**:1203–12.
7. Cerecedo D, Mondragon R, Cisneros B, Martinez-Perez F, Martínez-Rojas D, Rendón A. Role of dystrophins and utrophins in platelet adhesion process. *Br J Haematol* 2006;**134**:83–91.
8. Cerecedo D, Cisneros B, Gomez P, Galvan IJ. Distribution of dystrophin- and utrophin-associated protein complexes during activation of human neutrophils. *Exp Hematol* 2010;**38**:618–28 e613.
9. Park CY, Majeti R, Weissman IL. *In vivo* evaluation of human hematopoiesis through xenotransplantation of purified hematopoietic stem cells from umbilical cord blood. *Nat Protoc* 2008;**3**:1932–40.
10. Lambert M, Chafey P, Hugnot JP, Koulakoff A, Berwald-Netter Y, Billard C, Morris GE, Kahn A, Kaplan JC, Gilgenkrantz H. Expression of the transcripts initiated in the 62nd intron of the dystrophin gene. *Neuromuscul Disord* 1993;**3**:519–24.
11. Schofield JN, Blake DJ, Simmons C, Morris GE, Tinsley JM, Davies KE, Edwards YH. Apo-dystrophin-1 and apo-dystrophin-2, products of the Duchenne muscular dystrophy locus: expression during mouse embryogenesis and in cultured cell lines. *Hum Mol Genet* 1994;**3**:1309–16.
12. Rapaport D, Lederfein D, den Dunnen JT, Grootscholten PM, Van Ommen GJ, Fuchs O, Nudel U, Yaffe D. Characterization and cell type distribution of a novel, major transcript of the Duchenne muscular dystrophy gene. *Differentiation* 1992;**49**:187–93.
13. Lev AA, Feener CC, Kunkel LM, Brown RH Jr. Expression of the Duchenne's muscular dystrophy gene in cultured muscle cells. *J Biol Chem* 1987;**262**:15817–20.
14. Nudel U, Robzyk K, Yaffe D. Expression of the putative Duchenne muscular dystrophy gene in differentiated myogenic cell cultures and in the brain. *Nature* 1988;**331**:635–8.
15. Austin RC, Howard PL, D'Souza VN, Klamut HJ, Ray PN. Cloning and characterization of alternatively spliced isoforms of Dp71. *Hum Mol Genet* 1995;**4**:1475–83.
16. Wilson J, Putt W, Jimenez C, Edwards YH. Up71 and up140, two novel transcripts of utrophin that are homologues of short forms of dystrophin. *Hum Mol Genet* 1999;**8**:1271–8.
17. Gramolini AO, Jasmin BJ. Expression of the utrophin gene during myogenic differentiation. *Nucleic Acids Res* 1999;**27**:3603–9.
18. Fruehauf S, Srbic K, Seggewiss R, Topaly J, Ho AD. Functional characterization of podia formation in normal and malignant hematopoietic cells. *J Leukoc Biol* 2002;**71**:425–32.
19. Byers TJ, Lidov HG, Kunkel LM. An alternative dystrophin transcript specific to peripheral nerve. *Nat Genet* 1993;**4**:77–81.

 

20. Imamura M, Araishi K, Noguchi S, Ozawa E. A sarcoglycan-dystroglycan complex anchors Dp116 and utrophin in the peripheral nervous system. *Hum Mol Genet* 2000;**9**:3091–100.
21. Hnia K, Hugon G, Masmoudi A, Mercier J, Rivier F, Mornet D. Effect of beta-dystroglycan processing on utrophin/Dp116 anchorage in normal and mdx mouse Schwann cell membrane. *Neuroscience* 2006;**141**: 607–20.
22. Suda T, Arai F. Wnt signaling in the niche. *Cell* 2008; **132**:729–30.
23. Uchida Y, Maeda Y, Kimura E, Yamashita S, Nishida Y, Arima T, Hirano T, Uyama E, Mita S, Uchino M. Effective repetitive dystrophin gene transfer into skeletal muscle of adult mdx mice using a helper-dependent adenovirus vector expressing the coxsackie virus and adenovirus receptor (CAR) and dystrophin. *J Gene Med* 2005;**7**:1010–22.
24. Arai F, Hirao A, Ohmura M, Sato H, Matsuoka S, Takubo K, Ito K, Koh GY, Suda T. Tie2/angiopoietin-1 signaling regulates hematopoietic stem cell quiescence in the bone marrow niche. *Cell* 2004;**118**:149–61.
25. Yoshihara Y, Onodera H, Iinuma K, Itoyama Y. Abnormal kainic acid receptor density and reduced seizure susceptibility in dystrophin-deficient mdx mice. *Neuroscience* 2003;**117**:391–5.
26. Thompson O, Moore CJ, Hussain SA, Kleino I, Peckham M, Hohenester E, Ayscough KR, Saksela K, Winder SJ. Modulation of cell spreading and cell-substrate adhesion dynamics by dystroglycan. *J Cell Sci* 2010;**123**: 118–27.
27. Petersen BE, Grossbard B, Hatch H, Pi L, Deng J, Scott EW. Mouse A6-positive hepatic oval cells also express several hematopoietic stem cell markers. *Hepatology* 2003;**37**:632–40.
28. Gonzalez-Ramirez R, Morales-Lazaro SL, Tapia-Ramirez V, Mornet D, Cisneros B. Nuclear and nuclear envelope localization of dystrophin Dp71 and dystrophin-associated proteins (DAPs) in the C2C12 muscle cells: DAPs nuclear localization is modulated during myogenesis. *J Cell Biochem* 2008;**105**:735–45.
29. Artegiani B, Labbaye C, Sferra A, Quaranta MT, Torreri P, Macchia G, Ceccarini M, Petrucci TC, Macioce P. The interaction with HMG20a/b proteins suggests a potential role for beta-dystrobrevin in neuronal differentiation. *J Biol Chem* 2010;**285**:24740–50.
30. Dalloz C, Sarig R, Fort P, *et al*.. Targeted inactivation of dystrophin gene product Dp71: phenotypic impact in mouse retina. *Hum Mol Genet* 2003;**12**:1543–54.
31. Rivier F, Robert A, Hugon G, Mornet D. Different utrophin and dystrophin properties related to their vascular smooth muscle distributions. *FEBS Lett* 1997; **408**:94–8.

 